- Halogen Bonding inside a Molecular Container
  El-Sheshtawy, H. S.; Bassil, B. S.; Assaf, K.I.; Kortz, U.; Nau, W. M. *J. Am. Chem. Soc.* **2012**, *134*, 19935–19941.
  Abstract:

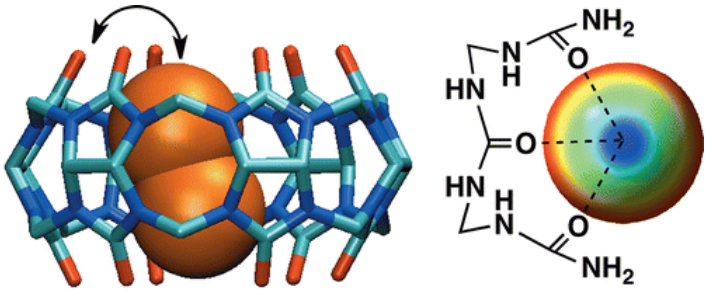

The synthetic macrocycle cucurbit[6]uril forms host–guest inclusion complexes with molecular dibromine and diiodine. As evidenced by their crystal structures, the encapsulated dihalogens adapt a tilted axial geometry and are held in place by two different types of halogen-bonding interactions, one with a water molecule (bond distances 2.83 Å for O···Br and 3.10 Å for O···I) and the other one with the ureido carbonyl groups of the molecular container itself (bond distances 3.33 Å for O···Br and 3.49 Å for O···I). While the former is of the conventional type, involving the lone electron pair of an oxygen donor, the latter is perpendicular, involving the π-system of the carbonyl oxygen (N–C═O···X dihedrals ca. 90°). Such perpendicular interactions resemble those observed in protein complexes of halogenated ligands. A statistical analysis of small-molecule crystal structural data, as well as quantum-chemical calculations with urea as a model (MP2/aug-cc-pVDZ-PP), demonstrates that halogen bonding with the π-system of the carbonyl oxygen can become competitive with the commonly favored lone-pair interaction whenever the carbonyl group carries electron-donating substitutents, specifically for ureas, amides, and esters, and particularly when the lone pairs are engaged in orthogonal hydrogen bonding (*h*X bonds). The calculations further demonstrate that the perpendicular interactions remain significantly attractive also for nonlinear distortions of the O···X–X angle to ca. 140°, the angle observed in the two reported crystal structures. The structural and theoretical data jointly support the assignment of the observed dihalogen–carbonyl contacts as genuine halogen bonds.

- Ion Permeation by a Folded Multiblock Amphiphilic Oligomer Achieved by Hierarchical Construction of Self-Assembled Nanopores
  Muraoka, T.; Shima, T.; Hamada, T.; Morita, M.; Takagi, M.; Tabata, K. V.; Noji, H.; Kinbara, K. *J. Am. Chem. Soc.* **2012**, *134*, 19788–19794.
  Abstract:

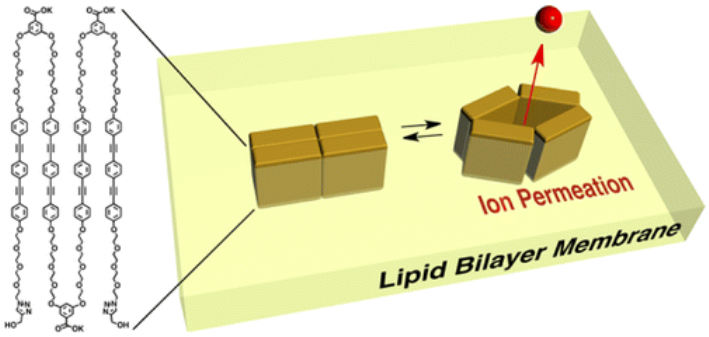

A multiblock amphiphilic molecule **1**, with a tetrameric alternating sequence of hydrophilic and hydrophobic units, adopts a folded structure in a liposomal membrane like a multipass

transmembrane protein, and is able to transport alkali metal cations through the membrane. Hill's analysis and conductance measurements, analyzed by the Hille equation, revealed that the tetrameric assembly of **1** forms a 0.53 nm channel allowing for permeation of cations. Since neither **3**, bearing flexible hydrophobic units and forming no stacked structures in the membrane, nor **2**, a monomeric version of **1**, is able to transport cations, the folded conformation of **1** in the membrane is likely essential for realizing its function. Thus, function and hierarchically formed higher-order structures of **1**, is strongly correlated with each other like proteins and other biological macromolecules.

- Synthesis, Characterization, and Computational Studies of Cycloparaphenylene Dimers
  Xia, J.; Golder, M. R.; Foster, M. E.; Wong, B. M.; Jasti, R. *J. Am. Chem. Soc.* **2012**, *134*, 19709–19715.
  Abstract:

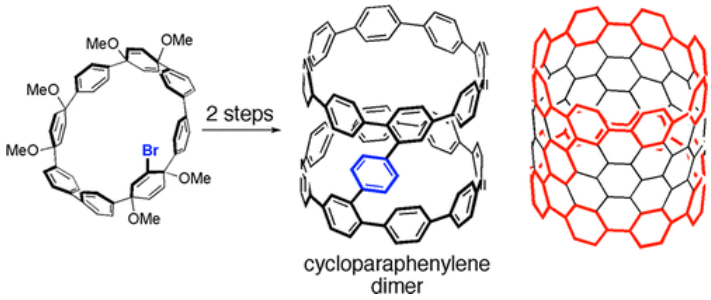

Two novel arene-bridged cycloparaphenylene dimers (**1** and **2**) were prepared using a functionalized precursor, bromo-substituted macrocycle **7**. The preferred conformations of these dimeric structures were evaluated computationally in the solid state, as well as in the gas and solution phases. In the solid state, the trans configuration of 1 is preferred by 34 kcal/mol due to the denser crystal packing structure that is achieved. In contrast, in the gas phase and in solution, the cis conformation is favored by 7 kcal/mol (dimer **1**) and 10 kcal/mol (dimer **2**), with a cis to trans activation barrier of 20 kcal/mol. The stabilization seen in the cis conformations is attributed to the increased van der Waals interactions between the two cycloparaphenylene rings. These calculations indicate that the cis conformation is accessible in solution, which is promising for future efforts toward the synthesis of short carbon nanotubes (CNTs) via cycloparaphenylene monomers. In addition, the optoelectronic properties of these dimeric cycloparaphenylenes were characterized both experimentally and computationally for the first time.

- Synthesis, Computed Stability, and Crystal Structure of a New Family of Inorganic Compounds: Carbonophosphates
  Chen, H.; Hautier, G.; Ceder, G. *J. Am. Chem. Soc.* **2012**, *134*, 19619–19627.
  Abstract:

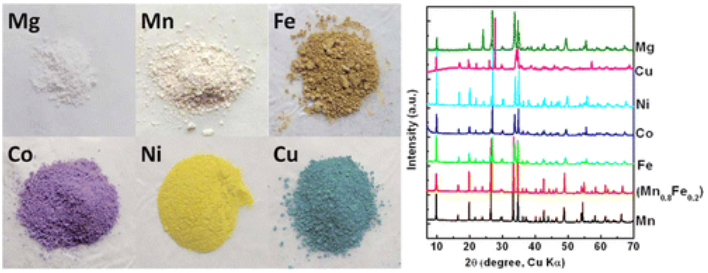

Ab initio-based high-throughput computing and screening are now being used to search and predict new functional materials and novel compounds. However, systematic experimental validation on the predictions remains highly challenging, yet desired. Careful comparison between computational predictions and experimental results is sparse in the literature. Here we report on a systematic experimental validation on previously presented computational predictions of a novel alkali carbonophosphate family of compounds. We report the successful hydrothermal synthesis and structural characterization of multiple sodium carbonophosphates. The experimental conditions for formation of the carbonophosphates and the computational results are compared and discussed. We also demonstrate topotactic chemical de-sodiation of one of the compounds, indicating the potential use of this novel class of compounds as Li+ or Na+ insertion electrodes.

- Engineering of Complex Order and the Macroscopic Deformation of Liquid Crystal Polymer Networks
  de Haan, L. T.; Sánchez-Somolinos, C.; Bastiaansen, C. M. W.; Schenning, A. P. H. J.; Broer, D. J. *Angew. Chem. Int. Ed.* **2012**, *51*, 12469–12472.
  Abstract:

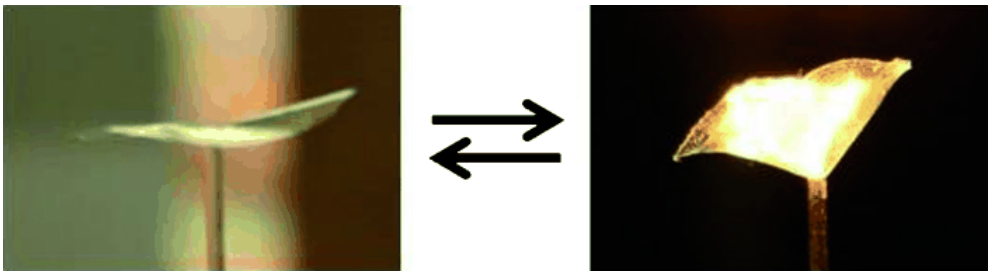

Rise or fall: Complex-structured freestanding polymer films with molecular order in three dimensions were prepared through photoalignment of polymerizable liquid crystals. The resulting films deform into cone and saddle shapes upon heating.

- Medication Detection by a Combinatorial Fluorescent Molecular Sensor
  Rout, B.; Unger, L.; Armony, G.; Iron, M. A.; Margulies, D. *Angew. Chem. Int. Ed.* **2012**, *51*, 12477–12481.
  Abstract:

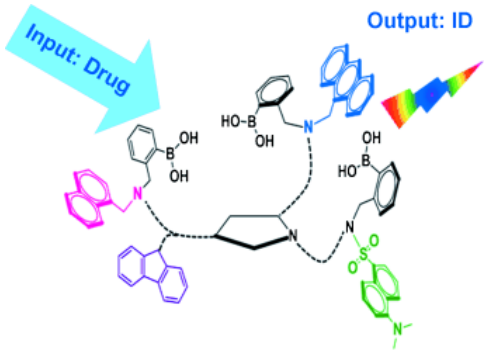

Working together to uncover the truth: A molecule-sized diagnostic system combining several recognition elements and four fluorescence-emission channels enabled the identification of a wide range of pharmaceuticals on the basis of distinct photophysical processes. The molecular sensor (see simplified representation; ID=identification) was also used to analyze drug concentrations and combinations in urine samples in a high-throughput manner.

- How Thiostrepton Was Made in the Laboratory
  Nicolaou, K. C. *Angew. Chem. Int. Ed.* **2012**, *51*, 12414–12436.
  Abstract:

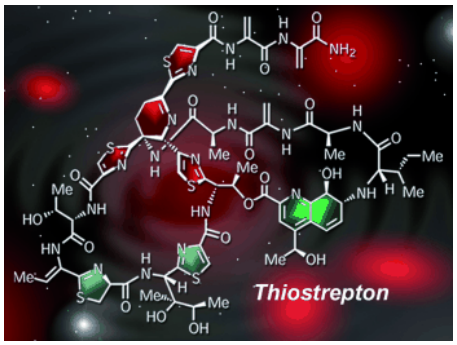

An adventurous undertaking: The synthetic conquest of thiostrepton was achieved in 2004. In this vivid account the author describes the laboratory odyssey with its many intriguing twists and turns that led to this memorable total synthesis**.**

- Double-Effector Nanoparticles: A Synergistic Approach to Apoptotic Hyperthermia
  Yoo, D.; Jeong, H.; Preihs, C.; Choi, J.-S.; Shin, T.-H.; Sessler, J. L.; Cheon, J. *Angew. Chem. Int. Ed.* **2012**, *51*, 12482–12485.
  Abstract:

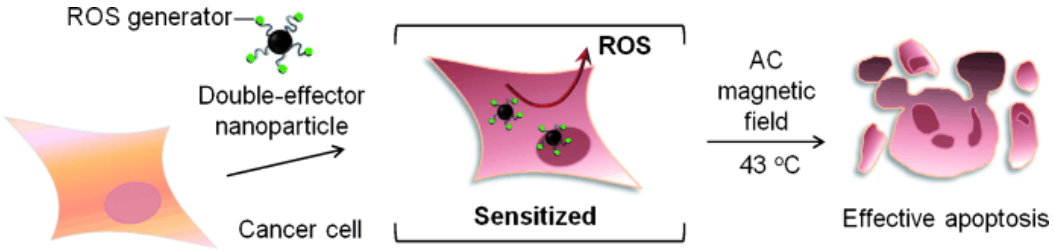

Highly efficient apoptotic hyperthermia is achieved using a double-effector nanoparticle that can generate reactive oxygen species (ROS) and heat. ROS render cancer cells more susceptible to subsequent heat treatment, which remarkably increases the degree of apoptotic cell death. Xenograft tumors (100 mm3) in mice are completely eliminated within 8 days after a single mild magnetic hyperthermia treatment at 43 °C for 30 min.

- A toolbox of differently sized and labeled PMMA nanoparticles for cellular uptake investigations
  Vollrath, A.; Schallon, A.; Pietsch, C.; Schubert, S.; Nomoto, T.; Matsumoto, Y.; Kataoka, K.; Schubert, U. S. *Soft Matter* **2013**, *9*, 99-108.
  Abstract:

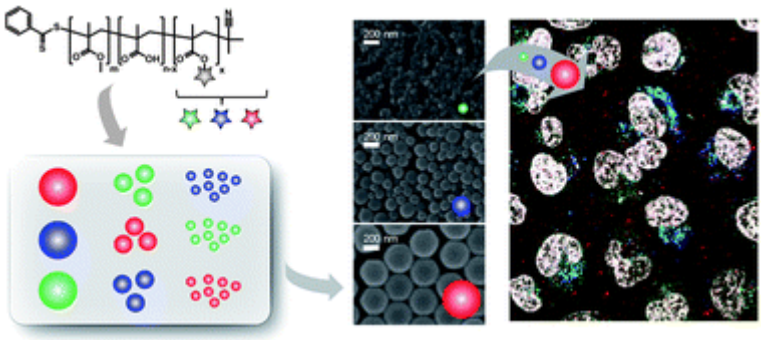

The cellular internalization of defined PMMA nanoparticles was investigated. For this purpose, the biocompatible copolymer p(MMA-*stat*-MAA)$_{0.91:0.09}$ was synthesized by RAFT polymerization and labeled with three different fluorescent dyes (λ_{Ex} = 493, 557, and 653 nm). Nanoparticles were formulated from the differently labeled copolymers into samples with relatively narrow size distribution (diameter d < 100 nm, 100 to 200 nm, >300 nm) under appropriate conditions of nanoprecipitation and were subsequently characterized by DLS and SEM. Mixtures of the differently sized nanoparticle samples were applied for internalization studies using monolayer cultured HeLa cells. The localization of the nanoparticles was detected after certain time points up to 24 h by CLSM, using LysoTracker as a marker for late endosomes and lysosomes. In investigations by flow cytometry, a fast uptake of medium sized nanoparticles was found, whereas the large and small nanoparticles exhibited a slower internalization. However, small and medium sized nanoparticles were detected in the late endosomes/lysosomes, whereas the large nanoparticles exhibit little co-localization with LysoTracker. Moreover, it could be shown by using different inhibitors for clathrin-dependent (chlorpromazine), caveolin-dependent (filipin III) endocytosis and macropinocytosis (EIPA) that nanoparticles with d < 200 nm were internalized *via* clathrin-dependent endocytosis, whereas those with d > 300 nm were internalized *via* macropinocytosis.

- Multiple stimuli-responsive polymeric micelles for controlled release
  Dong, J.; Wang, Y.; Zhang, J.; Zhan, X.; Zhu, S.; Yang, H.; Wang, G. *Soft Matter* **2013**, *9*, 370-373.
  Abstract:

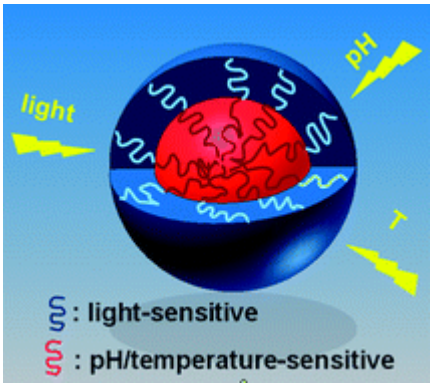

Multiple stimuli-responsive polymeric micelles that can respond to light, temperature and pH have been prepared by a novel polymer, pyrene-functionalized poly (dimethylaminoethyl methacrylate), where the pyrene-quaternized segments form a light-responsive shell and the unquaternized segments form a temperature/pH-responsive core. Under UV irradiation, the micelles could be dissociated; when the temperature increased above the lower critical solution temperature, the micelles shrunk. At pH 3, the micelles could be swelled/dissociated and at pH 10, the micelles could be collapsed to complex micelles. The controlled release of Nile Red from the micelle under stimuli was demonstrated. This novel multiple stimuli-responsive micelle shows potential as a new nanocarrier and delivery system.

- An Extremely Redox-Active Air-Stable Neutral π Radical: Dicyanomethylene-Substituted Triangulene with a Threefold Symmetry
  Ueda, A.; Wasa, H.; Nishida, S.; Kanzaki, Y.; Sato, K.; Shiomi, D.; Takui, T.; Morita, Y. *Chem. Eur. J.* **2012**, *18*, 16272–16276.
  Abstract:

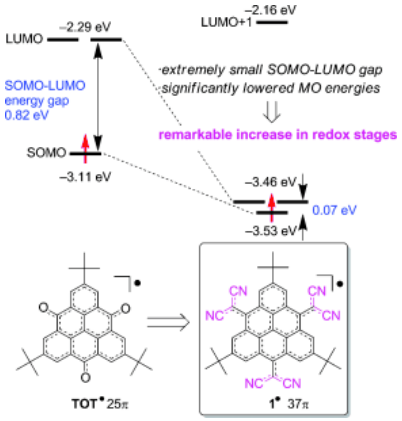

Radically active: A redox-active air-stable neutral π radical (1˙) with three dicyanomethylene groups introduced with threefold symmetry into a triangulene π skeleton instead of the oxygen atoms of TOT˙ was designed, synthesized, and characterized (see figure). The enhanced electron-accepting ability and extended π-electronic system of this chemical modification gave an extremely small SOMO–LUMO gap and significantly lowered the frontier orbital energies, leading to the remarkable increase in the redox stages.

- Synthesis and Immunological Evaluation of Self-Assembling and Self-Adjuvanting Tricomponent Glycopeptide Cancer-Vaccine Candidates
  Wilkinson, B. L.; Day, S.; Chapman, R.; Perrier, S.; Apostolopoulos, V.; Payne, R. J. *Chem. Eur. J.* **2012**, *18*, 16540–16548.
  Abstract:

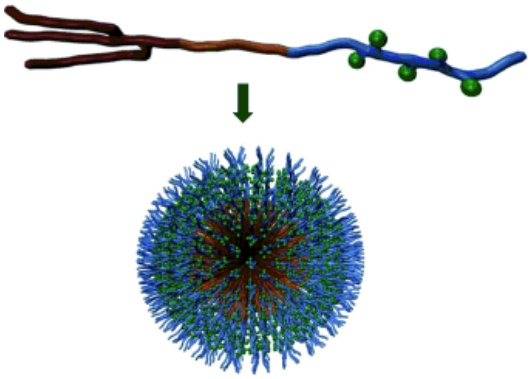

Just add water! The synthesis of a number of tricomponent glycopeptide cancer-vaccine candidates is described. These vaccines contain a tumor-associated peptide or glycopeptide antigen covalently linked to a universal T-cell helper peptide and an immunoadjuvant. These vaccines spontaneously self-assembled in aqueous media to form stable nanoparticles and elicited a strong humoral immune response in mice models without the addition of an external adjuvant.

- A 3D AgCl Hierarchical Superstructure Synthesized by a Wet Chemical Oxidation Method
  Lou, Z.; Huang, B.; Ma, X.; Zhang, X.; Qin, CX. Wang, Z.; Dai, Y.; Liu, Y. *Chem. Eur. J.* **2012**, *18*, 16090–16096.
  Abstract:

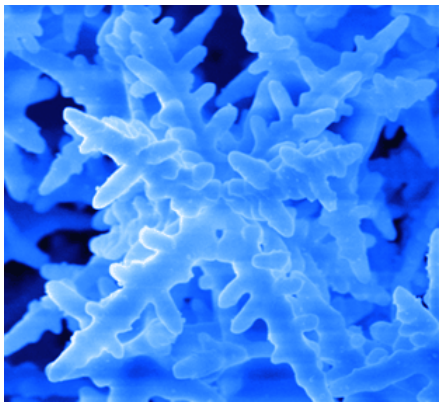

A novel 3D AgCl hierarchical superstructure, with fast growth along the 〈111〉 directions of cubic seeds, is synthesized by using a wet chemical oxidation method. The morphological structures and the growth process are investigated by scanning electron microscopy and X-ray diffraction. The crystal structures are analyzed by their crystallographic orientations. The surface energy of AgCl facets {100}, {110}, and {111} with absorbance of Cl^- ions is studied by density functional theory calculations. Based on the experimental and computational results, a plausible mechanism is proposed to illustrate the formation of the 3D AgCl hierarchical superstructures. With more active sites, the photocatalytic activity of the 3D AgCl hierarchical superstructures is better than those of concave and cubic ones in oxygen evolution under irradiation by visible light.

- Synthesis and Characterization of Reversible Chemosensory Polymers: Modulation of Sensitivity through the Attachment of Novel Imidazole Pendants
  Satapathy, R.; Padhy, H.; Wu, Y.-H.; Lin, H.-C. *Chem. Eur. J.* **2012**, *18*, 16061–16072.
  Abstract:

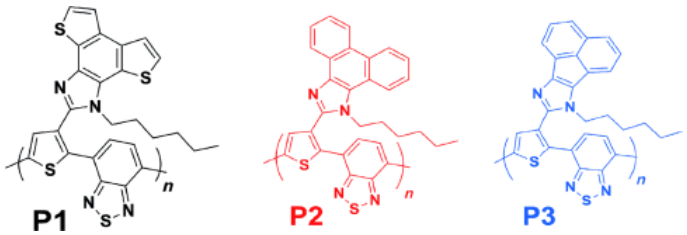

Three novel electron donor–acceptor conjugated polymers (**P1–P3**) bearing various imidazole pendants have been synthesized. Their excellent photophysical and electrochemical properties make them suitable transduction materials for chemosensing applications. Indeed, polymers **P1–P3** have been found to show remarkable sensing capabilities towards H^+ and Fe^{2+} in semi-aqueous solutions. Upon titration with H^+, polymers **P1** and **P2** showed hypsochromic shifts of their absorptions and photoluminescence (PL) maxima with enhanced fluorescence intensities. However, **P3** showed diminished absorption and fluorescence intensities under similar conditions due to static quenching. The anomalous behavior of **P3** compared with **P1** and **P2** has been clarified in terms of electronic distributions through computational analysis. Furthermore, **P3** (K_{SV}=1.03×10^7) showed a superior sensing ability towards Fe^{2+} compared with **P1**(K_{SV}=2.01×10^6) and **P2** (K_{SV}=4.12×10^6) due to its improved molecular wire effect. Correspondingly, the fluorescence lifetime of **P3** was greatly decreased (almost 11-fold) compared to those of polymers **P1** (4.6-fold) and **P2** (6.2-fold) in the presence of Fe^{2+}. By means of a fluorescence on-off-on approach, chemosensing reversibilities in protonation–deprotonation and metallation–demetallation have been achieved by employing triethylamine (TEA) and the disodium salt of ethylenediaminetetraacetic acid (Na_2-EDTA)/phenanthroline, respectively, as suitable counter ligands. ^{1}H NMR titrations have revealed the

unique behavior of **P3** compared with **P1** and **P2**. To the best of our knowledge, there have been no previous reports of Fe^{2+} sensors based on single imidazole receptors conjugated to a main-chain polymer showing such a diverse sensitivity pattern depending on their attached substituents.

- Size Does Matter: How To Control Organization of Organic Dyes in Aqueous Environment Using Specific Ion Effects
  Mooi, S. M.; Heyne, B. *Langmuir* **2012**, *28*, 16524–16530.
  Abstract:

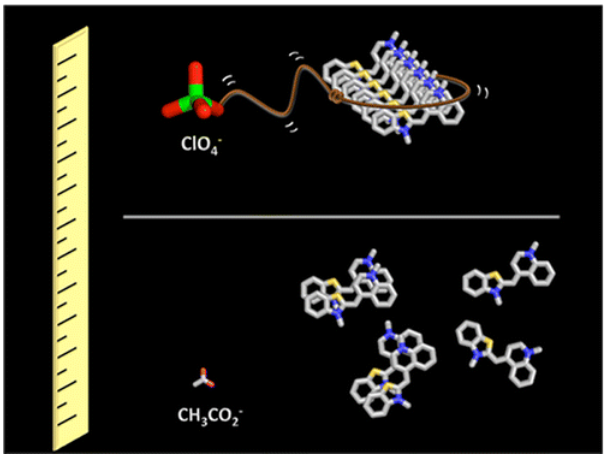

Understanding the role played by external factors on the organization of molecules has the potential to contribute greatly to fundamental research and applications in fields as diverse as nanotechnology, medicine, material chemistry, etc. Countless studies involve the organization of small organic molecules in environments rich in ionic species, yet their participation in molecular organization is often overlooked. Herein, we critically assess the organization in aqueous solution of the cationic cyanine dye, thiazole orange, in the presence of different monovalent sodium salts. Our findings clearly indicate that not all ions are identical with regards to the organization of thiazole orange molecules and specific ions effects are at play. The conventional Debye and Hückel model is not sufficient to explain our results, and the participation of ionic species in molecular organization is explained in terms of the recent theory of water matching affinity. Herein, by choosing the right counterion with the appropriate size, we have shown that it is possible to either induce a simple shift in the monomer–dimer equilibrium of thiazole orange or to turn on the formation of larger organized structures.

- Nanostructured Metal-Free Electrochemical Catalysts for Highly Efficient Oxygen Reduction
  Zheng, Y.; Jiao, Y.; Jaroniec, M.; Jin, Y.; Qiao, S. Z. *Small* **2012**, *8*, 3550–3566.
  Abstract:

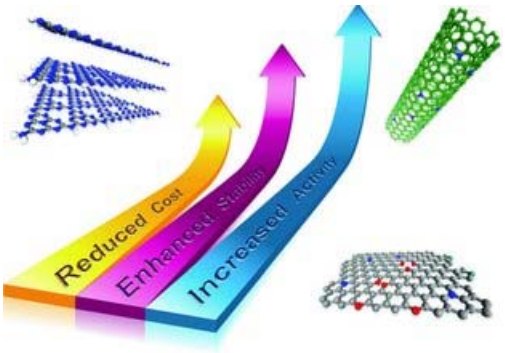

Replacing precious and nondurable Pt catalysts with cheap and commercially available materials to facilitate sluggish cathodic oxygen reduction reaction (ORR) is a key issue in the development of fuel cell technology. The recently developed cost effective and highly stable metal-free catalysts reveal comparable catalytic activity and significantly better fuel tolerance than that of current Pt-based catalysts; therefore, they can serve as feasible Pt alternatives for the next generation of ORR electrocatalysts. Their promising electrocatalytic properties and acceptable costs greatly promote the R&D of fuel cell technology. This review provides an overview of recent advances in state-of-the-art nanostructured metal-free electrocatalysts including nitrogen-doped carbons, graphitic-carbon nitride (g-C_3N_4)-based hybrids, and 2D graphene-based materials. A special emphasis is placed on the molecular design of these electrocatalysts, origin of their electrochemical reactivity, and ORR pathways. Finally, some perspectives are highlighted on the development of more efficient ORR electrocatalysts featuring high stability, low cost, and enhanced performance, which are the key factors to accelerate the commercialization of fuel cell technology.

- Peptides and peptidomimetics that behave as low molecular weight gelators
  Tomasini, C.; Castellucci, N. *Chem. Soc. Rev.* **2013**, *42*, 156-172.
  Abstract:

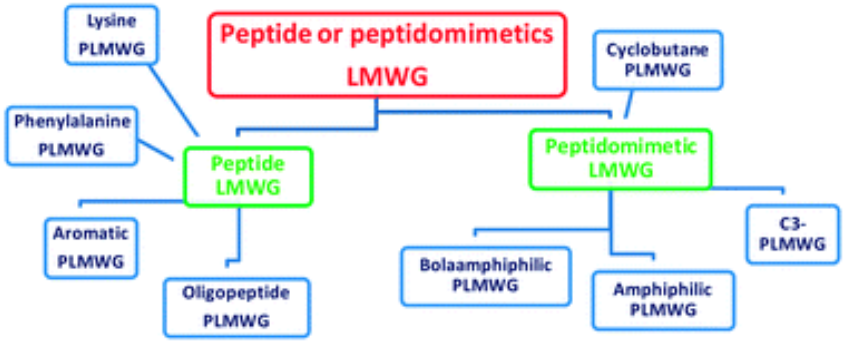

Gelators may be divided into chemical gels and physical gels: the internal structure of chemical gels is made of chemical bonds, while physical gels are characterized by dynamic cross-links that are constantly created and broken. The gelator present in physical gels may be an inorganic or an organic compound, the latter having a molecular weight of ≤500 amu. These compounds are generally called "low molecular weight gelators" (LMWGs). In this *tutorial review* we want to focus our attention on short peptides or peptidomimetics that behave as LMWGs. Peptidomimetics are small protein-like molecules designed to mimic natural peptides. To efficiently design a peptidomimetic, local constraints must be introduced into the skeleton, to induce the formation of preferred secondary structures.

- Biological applications of functionalized calixarenes
  Nimse, S. B.; Kim, T. *Chem. Soc. Rev.* **2013**, *42*, 366-386.
  Abstract:

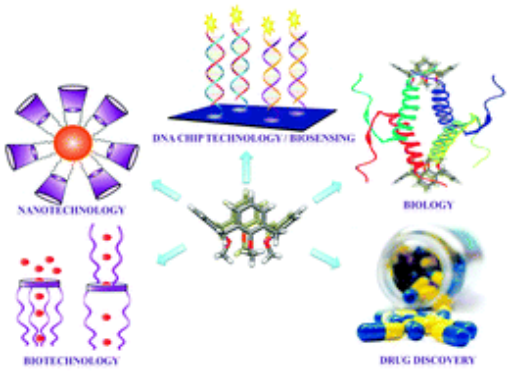

The functionalized calixarene derivatives exhibit remarkable properties towards organic and bioorganic molecules. However, the ability of calixarene derivatives to form stable complexes with biomolecules allows them to be applied for the development of biosensors and in the field of biology, biotechnology, and drug discovery. The applications of the functionalized calixarenes are summarized in this review, and an outlook for the future developments is discussed. A brief survey (of the last 10 years) on their biological application in various fields is also considered (199 references).

- Interior Engineering of a Viral Nanoparticle and Its Tumor Homing Properties
  Wen, A. M.; Shukla, S.; Saxena, P.; Aljabali, A. A. A.; Yildiz, I.; Dey, S.; Mealy, J. E.; Yang, A. C.; Evans, D. J.; Lomonossoff, G. P.; Steinmetz, N. F. *Biomacromolecules* **2012**, *13*, 3990–4001.
  Abstract:

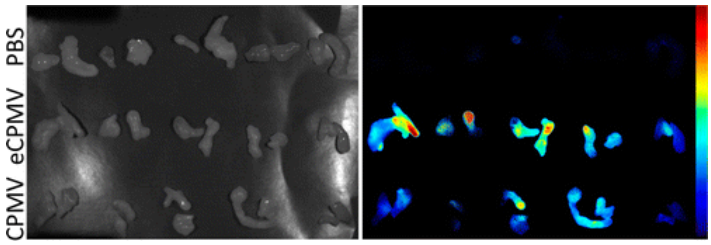

The development of multifunctional nanoparticles for medical applications is of growing technological interest. A single formulation containing imaging and/or drug moieties that is also capable of preferential uptake in specific cells would greatly enhance diagnostics and treatments. There is growing interest in plant-derived viral nanoparticles (VNPs) and establishing new platform technologies based on these nanoparticles inspired by nature.*Cowpea mosaic virus* (CPMV) serves as the standard model for VNPs. Although exterior surface modification is well-known and has been comprehensively studied, little is known of interior modification. Additional functionality conferred by the capability for interior engineering would be of great benefit toward the ultimate goal of targeted drug delivery. Here, we examined the capacity of empty CPMV (eCPMV) particles devoid of RNA to encapsulate a wide variety of molecules. We systematically investigated the conjugation of fluorophores, biotin affinity tags, large molecular weight polymers such as poly(ethylene glycol) (PEG), and various peptides through targeting reactive cysteines displayed selectively on the interior surface. Several methods are described that mutually confirm specific functionalization of the interior. Finally, CPMV and eCPMV were labeled with near-infrared fluorophores and studied side-by-side in vitro and in vivo. Passive tumor targeting via the enhanced permeability and retention effect and optical imaging were confirmed using a preclinical mouse model of colon cancer. The results of our studies lay the foundation for the development of the eCPMV platform in a range of biomedical applications.

- Covalent Cargo Loading to Molecular Shuttles via Copper-free "Click Chemistry"
  Früh, S. M.; Steuerwald. D.; Simon, U.; Vogel, V. *Biomacromolecules* **2012**, *13*, 3908–3911.
  Abstract:

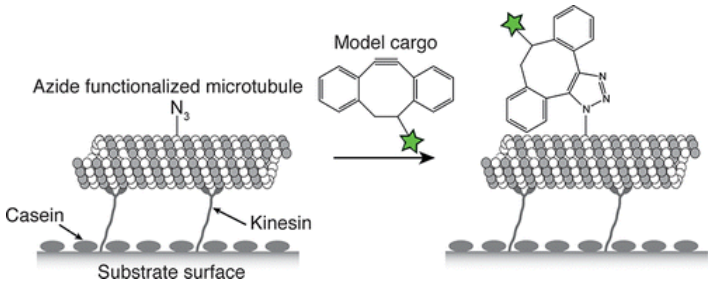

An important prerequisite for molecular shuttle-based functional devices is the development of adequate linker chemistries to load and transport versatile cargoes. Copper-free "click chemistry" has not been applied before to covalently load cargo onto molecular shuttles propelled by biological motors such as kinesin. Due to the high biocompatibility and bioorthogonality of the strain-promoted azide-alkyne cycloaddition, this approach has pronounced advantages compared to previous methods.

- Precision Synthesis of ω-Branch, End-Functionalized Comb Polystyrenes Using Living Anionic Polymerization and Thiol–Ene "Click" Chemistry
  Liu, B.; Quirk, R.-P.; Wesdemiotis, C.; Yol, A. M.; Foster, M. D. *Macromolecules* **2012**, *45*, 9233–9242.
  Abstract:

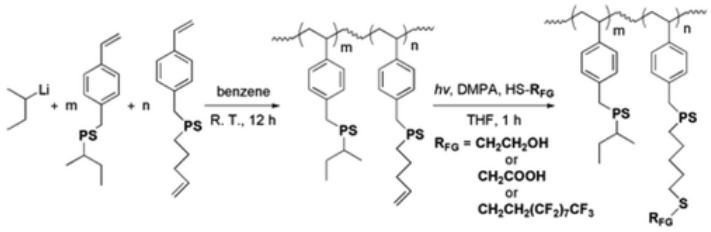

A combination of living anionic polymerization and thiol–ene "click" chemistry provides an efficient and convenient method for synthesis of well-defined comb polystyrenes with precisely controlled architecture details and a wide selection of functionalities. ω-(*p*-Vinylbenzyl)polystyrene macromonomer was synthesized by *sec*-butyllithium-initiated polymerization of styrene followed by termination with 4-vinylbenzyl chloride (VBC). For the synthesis of α-4-pentenyl-ω-(*p*-vinylbenzyl)polystyrene macromonomer, an unsaturated initiator, 4-pentenyllithium, was used followed by termination with VBC. To ensure successful living anionic polymerization of macromonomers, impurities present in the macromonomers and glass reactors were readily removed by titration with excess *sec*-butyllithium initiator right before initiation, resulting in polymacromonomers with controlled M_n (74 000, 130 000 g/mol) and narrow M_w/M_n. Living anionic copolymerization of mixtures of both types of macromonomers yielded a well-defined comb-shape precursor with controlled fractions of ω-vinyl branch end groups, which were subsequently subjected to facile and efficient functionalization by photoinitiated thiol–ene "click" reactions with diverse functional groups (−OH, $-CO_2H$, and $-C_8F_{17}$). Characterization by NMR, SEC, and MALDI-TOF mass spectrometry established their chemical structures and chain-end functionalities, which indicates precisely defined comb polystyrenes with controlled degrees of functionalization.

- Synthesis, Molecular and Photovoltaic Properties of Donor–Acceptor Conjugated Polymers Incorporating a New Heptacylic Indacenodithieno[3,2-*b*]thiophene Arene
  Chang, H. H.; Tsai, C.-E. ; Lai, Y.-Y. ; Chiou, D.-Y. ; Hsu, S.-L. ; Hsu, C.-S.; Cheng, Y.-J. *Macromolecules* **2012**, *45*, 9282–9291.
  Abstract:

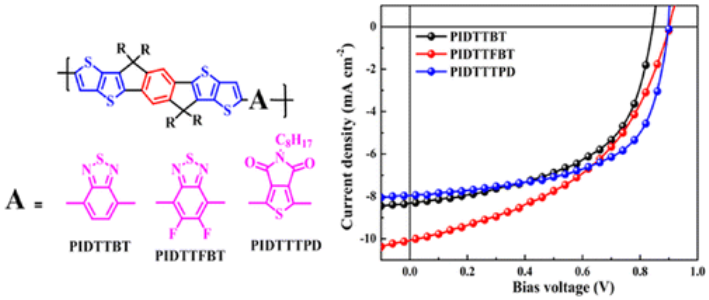

We have developed a new multifused indacenodithieno[3,2-*b*]thiophene arene (**IDTT**) unit where the central phenylene is covalently fastened with the two outer thieno[3,2-*b*]thiophene (**TT**) rings, forming two cyclopentadiene rings embedded in a heptacyclic structure. This rigid and coplanar **IDTT** building block was copolymerized with electron-deficient acceptors, 4,7-dibromo-2,1,3-benzothiadiazole (**BT**), 4,7-dibromo-5,6-difluoro-2,1,3-benzothiadiazole (**FBT**) and 1,3-dibromo-thieno[3,4-*c*]pyrrole-4,6-dione (**TPD**) via Stille polymerization, respectively. Because the higher content of the thienothiophene moieties in the fully coplanar **IDTT** structure facilitates π-electron delocalization, these new polymers show much improved light-harvesting abilities and enhanced charge mobilities compared to **PDITTBT** copolymer using hexacyclic diindenothieno[3,2-*b*]thiophene (**DITT**) as the donor moieties. The device using **PIDTTBT**:$PC_{71}BM$ (1:4, w/w) exhibited a decent power conversion efficiency (PCE) of 3.8%. Meanwhile, the solar cell using **PIDTTFBT**:$PC_{71}BM$ (1:4 in wt %) blend exhibited a greater V_{oc} value of 0.9 V and a larger J_{sc} of 10.08 mA/cm^2, improving the PCE to 4.2%. The enhanced V_{oc} is attributed to the lower-lying of HOMO energy level of **PIDTTFBT** as a result of fluorine withdrawing effect on the **BT** unit. A highest PCE of 4.3% was achieved for the device incorporating **PIDTTTPD**:$PC_{71}BM$ (1:4 in wt %) blend.

- Photostability of a dyad of magnesium porphyrin and fullerene and its application to photocurrent conversion
  Ichiki, T. ; Matsuo, Y.; Nakamura, E. *Chem. Commun.* **2013,** *49,* 279–281.
  Abstract:

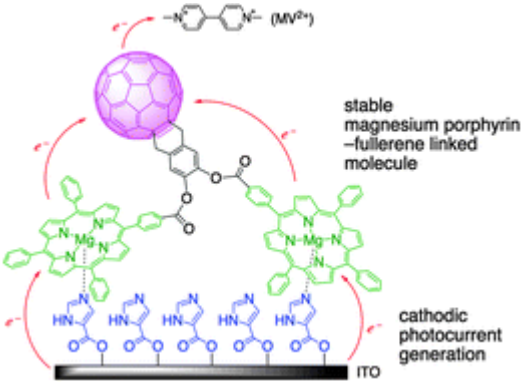

A new type of acceptor–donor$_2$ dyad system containing two magnesium porphyrin molecules and a fullerene molecule is much more stable than the magnesium porphyrin itself. When it is fabricated into a binary system using imidazole carboxylic acid as a linker to indium tin oxide, the molecule

effects efficient photocurrent generation that surpasses the device using the corresponding zinc porphyrin.

- A discrete octahedrally shaped $[Ag_6]^{4+}$ cluster encapsulated within silicotungstate ligands
  Kikukawa, Y.; Kuroda, Y.; Suzuki, K.; Hibino, M.; Yamaguchi, K.; Mizuno, N. *Chem. Commun.* **2013,** *49,* 376–378.
  Abstract:

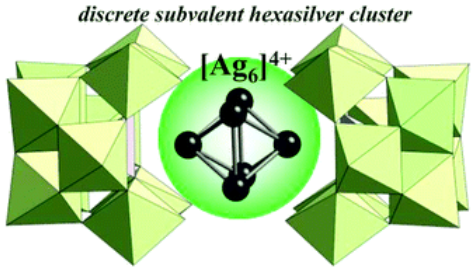

By the reaction of $TBA_4H_4[\gamma\text{-}SiW_{10}O_{36}]$ (TBA = tetra-*n*-butylammonium) with AgOAc (OAc = acetate) using dimethylphenylsilane as a reductant in acetone, a unique polyoxometalate containing a discrete octahedrally shaped $[Ag_6]^{4+}$ cluster, $TBA_8[Ag_6(\gamma\text{-}H_2SiW_{10}O_{36})_2]\cdot 5H_2O$, could be synthesized, and the molecular structure was determined.

- Transport Characteristics of Multichannel Transistors Made from Densely Aligned Sub-10 nm Half-Pitch Graphene Nanoribbons
  Liang, X.; Wi, S. *ACS Nano* **2012**, *6*, 9700-9710.
  Abstract:

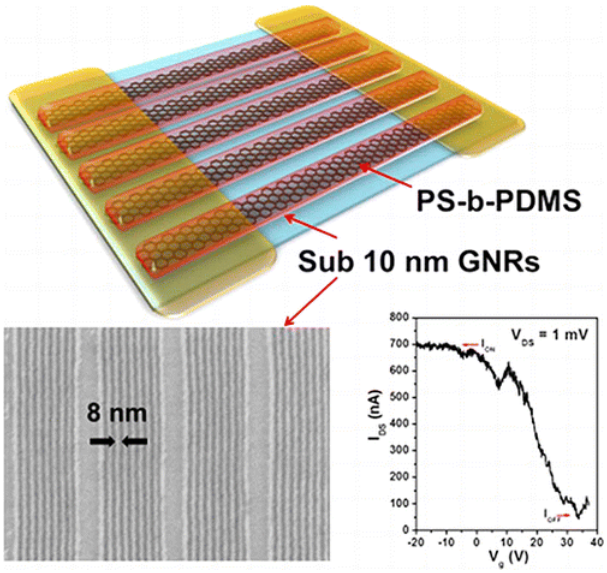

Densely aligned sub-10 nm graphene nanoribbons are desirable for scale-up applications in nanoelectronics. We implemented directed self-assembly of block-copolymers in combination with nanoimprint lithography to pattern sub-10 nm half-pitch nanoribbons over large areas. These graphene nanoribbons have the highest density and uniformity to date. Multichannel field-effect transistors were made from such nanoribbons, and the transport characteristics of transistors were studied. Our work indicates that a large ribbon-to-ribbon width variation in a multichannel FET can lead to nonsynchronized switching characters of multiple graphene channels and thus a poor ON/OFF

current ratio. Through process optimization, we have created 8 nm half-pitch graphene nanoribbons with the minimal ribbon-to-ribbon width variation of ≈2.4 nm (3σ value). The corresponding transistors exhibit an ON/OFF current ratio >10, which is among the highest values ever reported for transistors consisting of densely arranged graphene nanoribbons. This work provides important insights for optimizing the uniformity and transport properties of lithographically patterned graphene nanostructures. In addition, the presented fabrication route could be further developed for the scalable nanomanufacturing of graphene-based nanoelectronic devices over large areas.

- A Semiconducting Organic Radical Cationic Host–Guest Complex
  Fahrenbach, A. C.; Sampath, S.; Late, D. J.; Barnes, J. C.; Kleinman, S. L.; Valley, N.; Hartlieb, K. J.; Liu, Z.; Dravid, V. P.; Schatz, G. C.; Van Duyne, R. P.; Stoddart, J. F. *ACS Nano* **2012**, *6*, 9964-9971.
  Abstract:

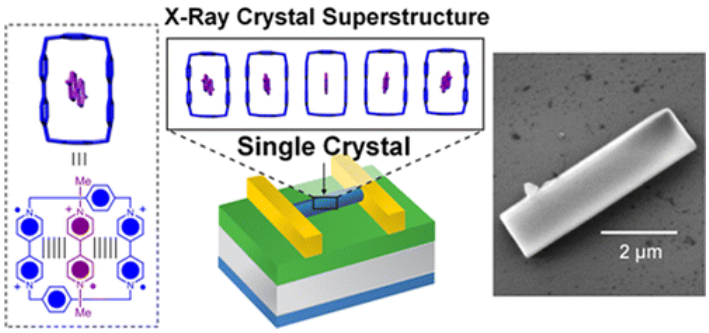

The self-assembly and solid-state semiconducting properties of single crystals of a trisradical tricationic complex composed of the diradical dicationic cyclobis(paraquat-*p*-phenylene) ($CBPQT^{2(\bullet+)}$) ring and methyl viologen radical cation ($MV^{\bullet+}$) are reported. An organic field effect transistor incorporating single crystals of the $CBPQT^{2(\bullet+)} \subset MV^{\bullet+}$ complex was constructed using lithographic techniques on a silicon substrate and shown to exhibit *p*-type semiconductivity with a mobility of 0.05 $cm^2\ V^{-1}\ s^{-1}$. The morphology of the crystals on the silicon substrate was characterized using scanning electron microscopy which revealed that the complexes self-assemble into "molecular wires" observable by the naked-eye as millimeter long crystalline needles. The nature of the recognition processes driving this self-assembly, radical–radical interactions between bipyridinium radical cations ($BIPY^{\bullet+}$), was further investigated by resonance Raman spectroscopy in conjunction with theoretical investigations of the vibrational modes, and was supported by X-ray structural analyses of the complex and its free components in both their radical cationic and dicationic redox states. These spectroscopic investigations demonstrate that the bond order of the $BIPY^{\bullet+}$ radical cationic units of host and guest components is not changed upon complexation, an observation which relates to its conductivity in the solid-state. We envision the modularity inherent in this kind of host–guest complexation could be harnessed to construct a library of custom-made electronic organic materials tailored to fit the specific needs of a given electronic application.

- Two-Stage Amplification of Receptors Using a Multilevel Orthogonal/Simultaneous Dynamic Combinatorial Library
  Escalante, A. M.; Orrillo, A. G.; Cabezudo, I.; Furlan, R. L. E. *Org. Lett.* **2012**, *14*, 5816–5819.
  Abstract:

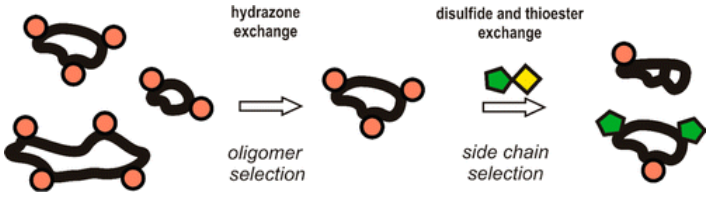

Sequential activation of different reversible exchange reactions in a dynamic combinatorial library allows directed exploration of the chemical space: initially a macrocyclic scaffold is selected by the template and finally side chain and conformational constrains are introduced into such a scaffold.

- A Switchable Ferrocene-Based [1]Rotaxane with an Electrochemical Signal Output
  Li, H.; Zhang, H.; Zhang, Q.; Zhang, Q.-W.; Qu, D.-H. *Org. Lett.* **2012**, *14*, 5900–5903.
  Abstract:

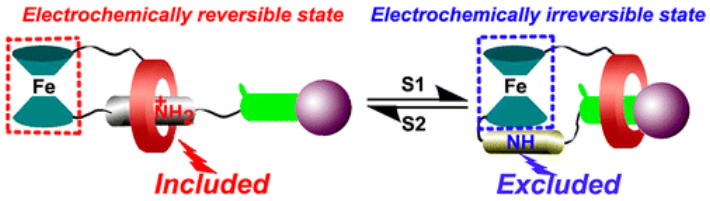

A [1]rotaxane, in which a linear rod is attached to one cyclopentadienyl (Cp) ring of a ferrocene unit and threaded into a dibenzo-24-crown-8 connected to the other Cp ring, was prepared. The mechanical motion of the rod-like part relative to the macrocycle has been demonstrated using 1H NMR spectroscopy. Cyclic voltammetry (CV) showed that the system can be chemically switched between electrochemically reversible and irreversible states, depending on the inclusion and exclusion of the ammonium/amine group from the macrocycle.

- High-density integration of carbon nanotubes via chemical self-assembly
  Park, H.; Afzali, A.; Han, S-J.; Tulevski, G. S.; Franklin, A. D.; Tersoff, J.; Hannon, J. B.; Haensch, W. *Nature Nanotechnology* **2012**, *7*, 787–791.
  Abstract:

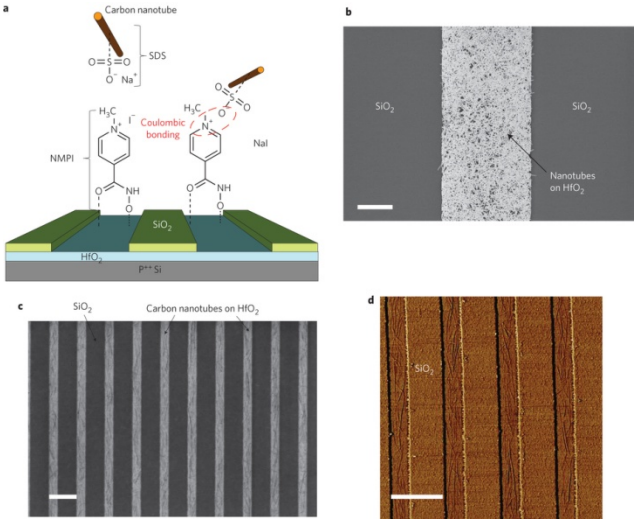

Carbon nanotubes have potential in the development of high-speed and power-efficient logic applications. However, for such technologies to be viable, a high density of semiconducting nanotubes must be placed at precise locations on a substrate. Here, we show that ion-exchange chemistry can be used to fabricate arrays of individually positioned carbon nanotubes with a density as high as 1 × 109 cm−2—two orders of magnitude higher than previous reports8, 9. With this

approach, we assembled a high density of carbon-nanotube transistors in a conventional semiconductor fabrication line and then electrically tested more than 10,000 devices in a single chip. The ability to characterize such large distributions of nanotube devices is crucial for analysing transistor performance, yield and semiconducting nanotube purity.

- A nanocomposite ultraviolet photodetector based on interfacial trap-controlled charge injection
  Guo, F.; Yang, B.; Yuan, Y.; Xiao, Z.; Dong, Q.; Bi Y.; Huang, J. *Nature Nanotechnology* **2012**, *7*, 798–802.
  Abstract:

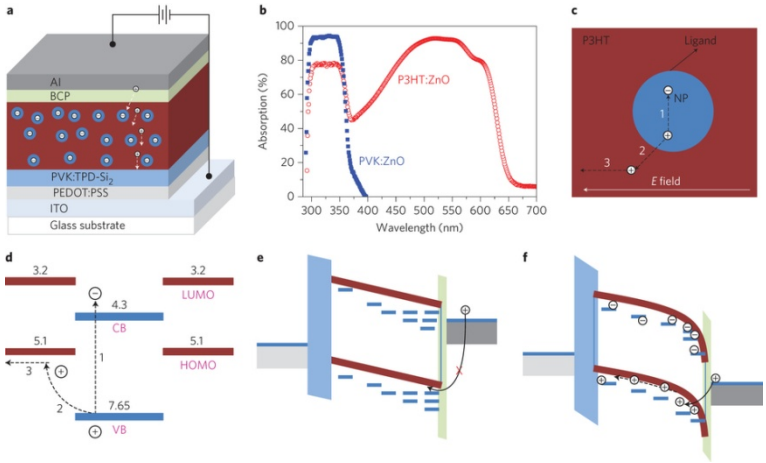

Ultraviolet photodetectors have applications in fields such as medicine, communications and defence, and are typically made from single-crystalline silicon, silicon carbide or gallium nitride p–n junction photodiodes. However, such inorganic photodetectors are unsuitable for certain applications because of their high cost and low responsivity (<0.2 A W−1)2. Solution-processed photodetectors based on organic materials and/or nanomaterials could be significantly cheaper to manufacture, but their performance so far has been limited. Here, we show that a solution-processed ultraviolet photodetector with a nanocomposite active layer composed of ZnO nanoparticles blended with semiconducting polymers can significantly outperform inorganic photodetectors. As a result of interfacial trap-controlled charge injection, the photodetector transitions from a photodiode with a rectifying Schottky contact in the dark, to a photoconductor with an ohmic contact under illumination, and therefore combines the low dark current of a photodiode and the high responsivity of a photoconductor (~721–1,001 A W−1). Under a bias of <10 V, our device provides a detectivity of 3.4 × 1015 Jones at 360 nm at room temperature, which is two to three orders of magnitude higher than that of existing inorganic semiconductor ultraviolet photodetectors.

- Phosphoryl/Sulfonyl-Substituted Iridium Complexes as Blue Phosphorescent Emitters for Single-Layer Blue and White Organic Light-Emitting Diodes by Solution Process
  Fan, C.; Li, Y.; Yang, C.; Wu, H.; Qin, J.; Cao, Y. *Chem. Mater.* **2012**, *24*, 4581–4587.
  Abstract:

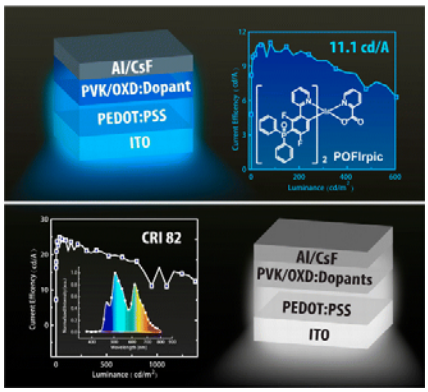

Two new phosphoryl/sulfonyl-substituted iridium complexes, POFIrpic and SOFIrpic, have been designed and synthesized on the basis of the structural frame of sky-blue FIrpic. The introduction of phosphoryl/sulfonyl moieties into the 5′-position of phenyl ring makes the emission peak blue-shift to the 460 nm, simultaneously the compounds maintain high photoluminescence quantum yields (PLQYs) of about 50% in solution. Single-layer blue and white polymer organic light-emitting diodes by full solution-process were fabricated with the following configuration: ITO/PEDOT:PSS/PVK:OXD-7:dopants/CsF/Al. The blue device based on POFIrpic shows a maximum current efficiency of 11.1 cd A^{-1}, a maximum external quantum efficiency of 7.1%, which are the highest ever reported for blue PhOLEDs by full solution process. The white device with POFIrpic as blue component reveals a maximum current efficiency of 25 cd A^{-1}, a maximum external quantum efficiency of 15%, and a good CRI value of 82.

- Hydrazine-Processed Ge-Substituted CZTSe Solar Cells
  Bag, S.; Gunawan, O.; Gokmen, W.; Zhu, Y.; Mitzi, D. B. *Chem. Mater.* **2012**, *24*, 4588–4593.
  Abstract:

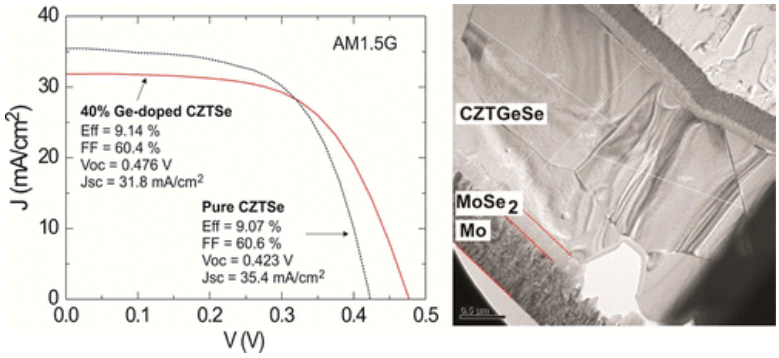

The p-type $Cu_2ZnSn(SxSe_{1-x})_4$ (with $x \approx 0$; CZTSe) thin-film solar cell absorber, made from earth-abundant elements, was substituted with Ge using a hydrazine-based mixed particle-solution approach for the film deposition. The crystallographic unit cell parameters of the absorber layer decrease with gradual incorporation of Ge. A solar cell fabricated from a 40% Ge-substituted absorber showed a 9.1% power conversion efficiency, a higher open-circuit voltage, and a wider band gap compared with the device based on the unsubstituted absorber layer. This result shows the possibility of substituting, using the hydrazine-processing approach, the metal site of CZTSe with Ge for further device optimization. One area for further improvement in the substituted absorber layer devices includes reduction of a ZnSe secondary phase, which was apparent in the higher-Ge-content films.